

Efficient Prostate Cancer Therapy with Tissue-Specific Homing Peptides Identified by Advanced Phage Display Technology

Akinori Wada,^{1,2} Tomoya Terashima,² Susumu Kageyama,¹ Tetsuya Yoshida,¹ Mitsuhiro Narita,¹ Akihiro Kawauchi,¹ and Hideto Kojima²

¹Department of Urology, Shiga University of Medical Science, Shiga, Japan; ²Department of Stem Cell Biology and Regenerative Medicine, Shiga University of Medical Science, Shiga, Japan

Selective targeting of drugs to tumor cells is a key goal in oncology. Here, we performed an *in vivo* phage display to identify peptides that specifically target xenografted prostate cancer cells. This yielded three peptide candidates, LN1 (C-TGTPARQ-C), LN2 (C-KNSMFAT-C), and LN3 (C-TNKHSPK-C); each of these peptides was synthesized and evaluated for binding and biological activity. LN1 showed the highest avidity for LNCaP prostate cancer cells *in vitro* and was thus administered to tumor-bearing mice to evaluate *in vivo* binding. Strikingly, LN1 specifically bound to the tumor tissue and exhibited very low reactivity with normal liver and kidney tissues. To demonstrate that LN1 could specifically deliver drugs to prostate cancer tissue, a therapeutic peptide, LNI-KLA (C-TGTPARQ-C-GGG-D₂[KLAKLAK]₂), was prepared and used to treat LNCaP cells *in vitro* and was also administered to tumor-bearing mice. The therapeutic peptide significantly suppressed growth of the cells both *in vitro* and *in vivo*. Our study shows that a selective homing peptide strategy could facilitate cell-specific targeting of therapeutics while avoiding adverse reactions in normal tissues.

INTRODUCTION

Although several therapeutic options are available to treat localized prostate cancer, metastatic disease is associated with a poor prognosis in prostate cancer patients. Currently, androgen deprivation therapy is the standard treatment for metastatic prostate cancer.¹ Despite the initial favorable response, many patients die once castration-resistant disease emerges.² The development of novel drugs, such as abiraterone, enzalutamide, and cabazitaxel, has improved survival to some extent.^{3–6} However, in many instances, treatment has to be discontinued due to the appearance of systemic adverse reactions. To overcome the limitations of these current therapies, there is a pressing need for a treatment strategy that allows selective targeting of cancer tissue while avoiding adverse effects on non-target tissues.

Homing peptides capable of selectively delivering many kinds of molecules have been identified and hold great promise for the development of less toxic therapeutic methods to treat several diseases.^{7–10}

These homing peptides usually consist of 3–12 amino acids with exceptionally strong binding affinity and selectivity for their target molecules.^{11,12} These peptides can be screened using phage display technology, which is an efficient method for searching a peptide library in order to identify a sequence that specifically binds to a target molecule.^{13,14} The method can be used both *in vitro* and *in vivo*;^{15,16} the latter approach allows the identification of homing peptides that target the surface of cells in their physiological microenvironment.^{12,16–21} Combining these homing peptides with an anticancer agent promotes more effective tumor regression than use of the anticancer agent alone.¹⁸ In addition, conjugation of these peptides to pro-apoptotic peptide sequences can be used to selectively induce cancer cell death.¹⁹

The existing *in vivo* phage display technology is problematic, as it does not consistently identify peptides that discriminate disease tissue from normal tissue.^{22,23} We designed the current study to address this issue. Specifically, we performed an initial phage display that identified peptides that did not bind to host tissues; this library subgroup was then used to identify peptides that homed to prostate cancer cells. Furthermore, in order to minimize toxicity to human normal tissues, we performed phage display on a cynomolgus monkey in addition to normal mice to collect phage populations that did not bind to non-diseased organs. Our approach provides an advanced strategy to isolate non-toxic homing peptides that specifically bind to cancer cells.

RESULTS

Identification of Prostate Cancer Homing Peptides Using *In Vivo* Phage Display

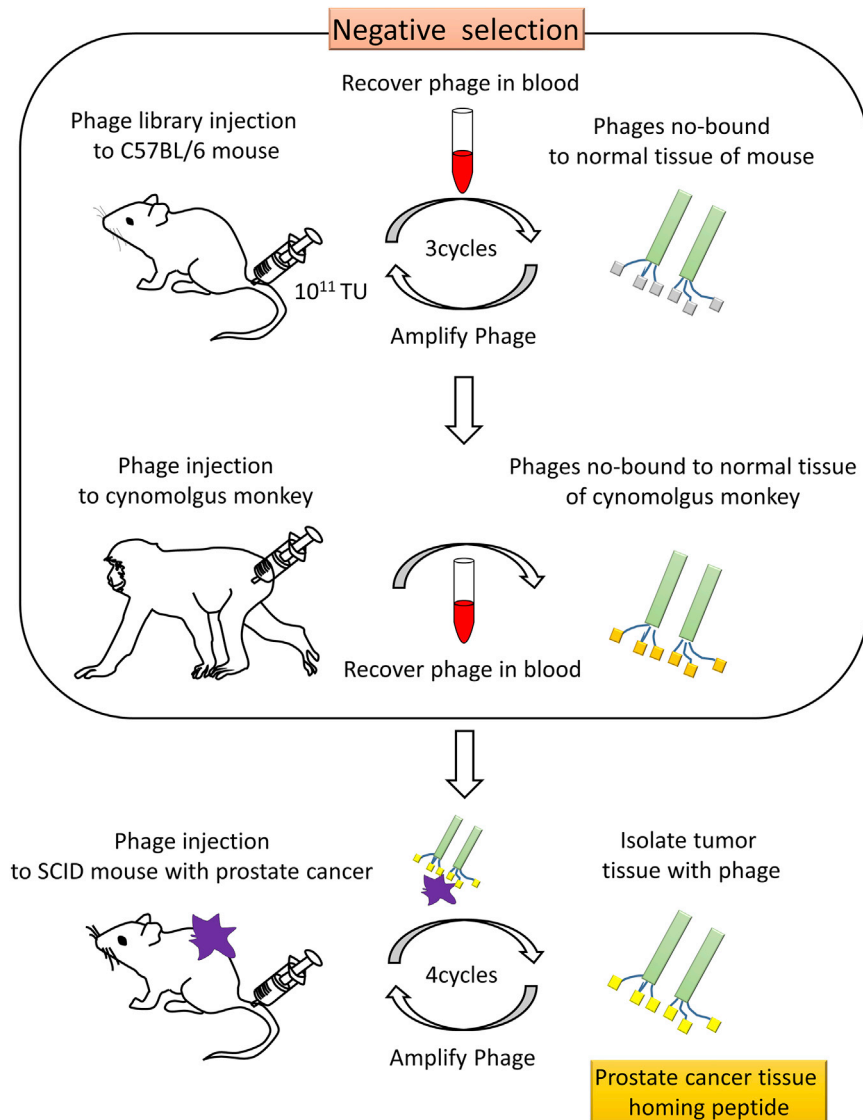
To exclude phage binding to normal tissues, we used blood as the source of peptides that did not bind to systemic organs. Three

Received 10 December 2018; accepted 10 January 2019;
<https://doi.org/10.1016/j.omto.2019.01.001>.

Correspondence: Tomoya Terashima, Department of Stem Cell Biology and Regenerative Medicine, Shiga University of Medical Science, Seta Tsukinowa-cho, Otsu 520-2192, Japan.

E-mail: tom@belle.shiga-med.ac.jp





rounds of *in vivo* phage display in mice and one round of *in vivo* phage display in a cynomolgus monkey were performed to collect this “negative” phage population (Figure 1). The DNA sequences of the isolates were analyzed; this confirmed that phage diversity was maintained (data not shown). A similar DNA analysis was performed after completion of four rounds of *in vivo* phage display in severe combined immunodeficient (SCID) mice with prostate cancer tissue transplantation (Figure 1). Thirty-two sequences, indicative of high-affinity binding peptides, were identified in this manner (Table 1). LN1 (C-TGTPARQ-C) and LN2 (C-KNSMFAT-C) peptides were the most frequent among the 32 candidate peptides and were found in 4 of 47 phage plaques (frequency, 8.5%) (Table 1). LN3 (C-TNKHSPK-C) and LN4 (C-SPKNILH-C) peptides were the next most frequent and were observed in 3 of 47 phage plaques (frequency, 6.4%) (Table 1). Due to their occurrence at high frequency, LN1, LN2, and LN3

optimal homing peptide for specific binding to prostate cancer tissue.

***In Vivo* Targeting of LN1, LN2, and LN3 Homing Peptides to Prostate Cancer**

LN1, LN2, and LN3 peptides were individually administered to SCID mice harboring subcutaneous LNCaP transplants and 3,3-diaminobenzidine (DAB) staining was performed to evaluate the extent of binding to tumor tissues and other major organs with high blood perfusion rates, such as liver and kidney. While LN1, LN2, and LN3 peptides bound to tumor tissue, the control peptide showed negligible binding (Figure 3). Strikingly, the LN1 and LN2 peptides did not bind to the liver or kidney tissue (Figure 3). Although the peptide showed a small but significant amount of binding to the kidney tissue, it did not bind to the liver (Figure 3). On the other hand, the control peptide bound to both liver and kidney tissue (Figure 3).

Figure 1. Schematic Representation of the Advanced Screening Procedure to Identify Homing Peptides Targeting Prostate Cancer

Negative selection: an *in vivo* phage display was performed to collect non-binding phages to normal tissues in mice (upper) and a cynomolgus monkey (middle). After negative selection, specific peptides homing to the cancer cells were identified by *in vivo* phage display in SCID mice bearing tumor xenografts (lower). TU, titer unit.

were selected as candidate prostate cancer homing peptides for further experiments.

Binding Affinity of LN1, LN2, and LN3 Peptides to Cancer Cells

To examine differences in the binding affinity of LN1, LN2, and LN3 peptides to cancer cells, each peptide was synthesized and conjugated with biotin at the N terminus before incubation with LNCaP cells for 24 h. Rhodamine (tetramethylrhodamine isothiocyanate [TRITC]) avidin D was applied and the binding ratio of LN1-LN3 peptides to LNCaP prostate cancer cells was calculated (Figure 2). Most of the cells were labeled with all three peptides (Figure 2A), whereas the control peptide (C-GPRTQTA-C, a scrambled sequence of the LN1 peptide) showed negligible signal (data not shown). The proportion of LN1 peptide bound to tumor cells was 95.1% (Figure 2B). In contrast, the binding of LN2 and LN3 peptides were 86.4% and 66.7%, respectively (Figure 2B). Fluorescent immunostaining also confirmed that LN1 bound the most avidly to tumor cells (Figure 2C). We thus conclude that the LN1 peptide is the most

Table 1. Amino Acid Sequence and Phage Plaque Frequencies of Peptides That Specifically Home on Prostate Cancer Cells

Amino Acid Sequence	Frequency	
LN1	C-TGTPARQ-C	4/47
LN2	C-KNSMFAT-C	4/47
LN3	C-TNKHSPK-C	3/47
LN4	C-SPKNILH-C	3/47
LN5	C-FPSPTRT-C	2/47
LN6	C-NAGTLGR-C	2/47
LN7	C-NKEFASQ-C	2/47
LN8	C-NSANNRI-C	2/47
LN9	C-STQSTTS-C	2/47
LN10	C-APPGKSE-C	1/47
LN11	C-APKNILH-C	1/47
LN12	C-APSSAT-C	1/47
LN13	C-ESKTPKN-C	1/47
LN14	C-FDHHTNS-C	1/47
LN15	C-GTRETLS-C	1/47
LN16	C-HAALNRS-C	1/47
LN17	C-HHSNQRQ-C	1/47
LN18	C-HRPDTRS-C	1/47
LN19	C-NRESPHL-C	1/47
LN20	C-NSRSHAI-C	1/47
LN21	C-PMPSTSY-C	1/47
LN22	C-PVTSRSD-C	1/47
LN23	C-RAWNEAP-C	1/47
LN24	C-SDRGLPS-C	1/47
LN25	C-SSKSDHS-C	1/47
LN26	C-TAYPAKA-C	1/47
LN27	C-TGAPARW-C	1/47
LN28	C-TKTGLHI-C	1/47
LN29	C-TSTAPLK-C	1/47
LN30	C-VTSPFHN-C	1/47
LN31	C-YSPRGGC-C	1/47
LN32	C-YTNPDNV-C	1/47

Given the results of the *in vitro* and *in vivo* experiments, we selected LN1 for further experiments to determine its potential utility for treatment of prostate cancer.

LN1 Homing Peptides Localize to Prostate Cancer Cells *In Vivo*

We performed fluorescent staining to determine the localization of LN1 in each tissue. The LN1 peptide displayed strong localization to tumor tissue, whereas the control peptide exhibited little binding (Figures 4A and 4B). Moreover, binding of LN1 to tissues in major organs such as the liver and kidney was much lower than that observed with the control peptide (Figure 4B). Colocalization of LN1 with prostate-specific antigen (PSA) anti-

body confirmed that the peptide was bound to tumor cells (Figure 5).

LNCaP Proliferation Is Inhibited by an LN1-Pro-apoptotic Peptide Fusion

To ascertain whether homing peptides have potential as vehicles for targeted drug delivery therapy, we determined whether a fusion construct composed of the pro-apoptotic peptide ₁₅(KLAKLAK)₂ and the LN1 peptide could induce death in LNCaP cells. The pro-apoptotic peptide is known to cause mitochondrial disruption and induce apoptotic cell death. No change in cell morphology was observed following treatment with control-KLA peptide or KLA peptide, but significant cell death was induced by the LN1-KLA peptide (Figure 6A). Proliferation was inhibited by 25 μ M LN1-KLA peptide but not by the same concentration of control-KLA peptide or KLA peptide (Figure 6B).

LN1-Apoptosis Fusion Peptide Inhibits the Growth of Prostate Cancer Xenografts

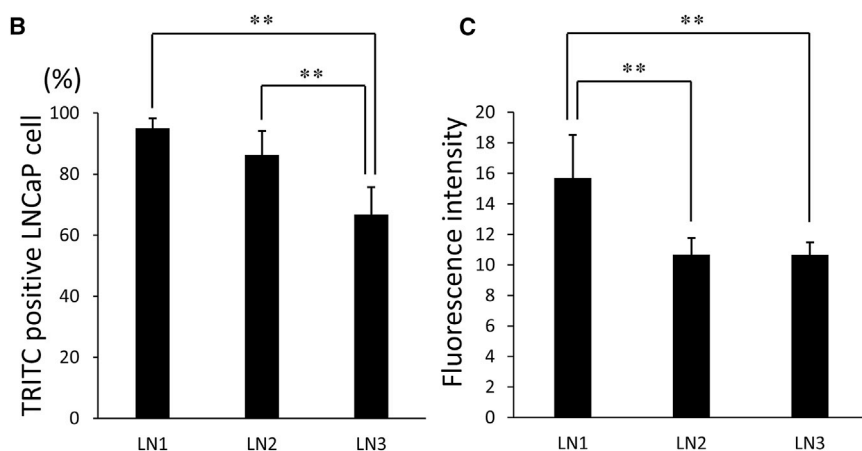
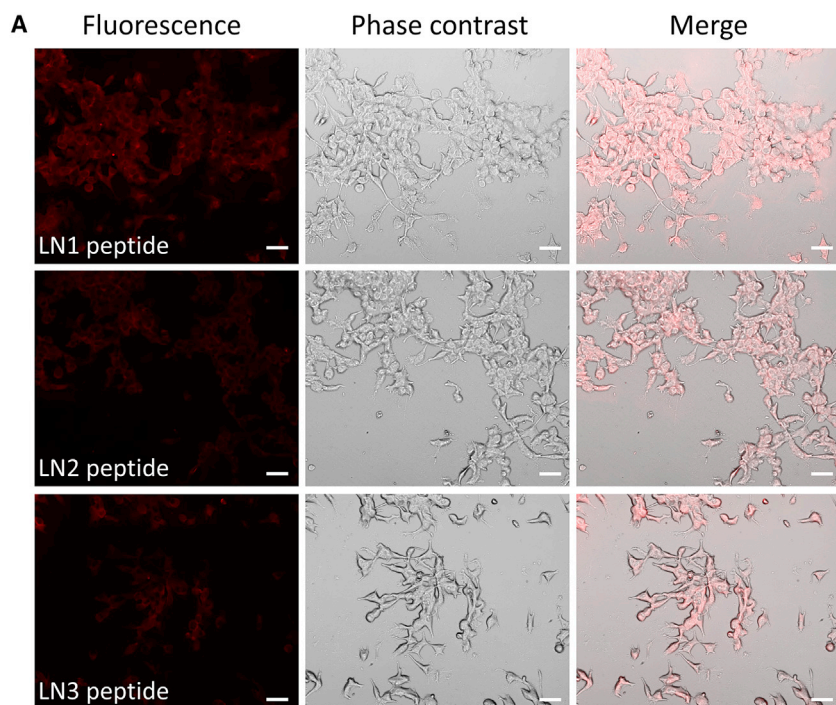
Following *in vivo* administration of phosphate-buffered saline (PBS), KLA-peptide, or control-KLA, the tumors displayed heterogeneity in ultrasound imaging (Figure 7A), indicating that viability was not affected. On the other hand, the LN1-KLA peptide induced tumor homogeneity, which was indicative of apoptosis or necrosis (Figure 7A). Whereas the tumors in control-treated mice grew 2-fold over the 22-day period, growth was reduced to 1.4-fold in mice treated with LN1-KLA peptide (Figure 7B).

DISCUSSION

In this study, we used phage display technology to identify a homing peptide that targets human LNCaP xenografts. The LNCaP cell line isolated from a lymph node metastasis from a prostate cancer patient.^{24,25} It expresses relevant markers of prostate cancer cells, such as PSA, prostate-specific membrane antigen, androgen receptor, and prostatic acid phosphatase.^{24,25} Indeed, our primary motivation for using this cell line was to provide proof of principle that earlier stages of metastatic prostate cancer could be treated by using homing peptides.

In vitro and *in vivo* phage displays have previously identified specific peptides that selectively bind to prostate cancer cell lines.^{26,27} However, peptides identified using *in vitro* phage display may not actually reach tumor cells in an *in vivo* context. To overcome this issue, we decided to perform *in vivo* phage displays and isolate sequence that were present in the blood, since by definition these represent peptides that can pass through the general circulation.

In 2006, Newton et al.²² identified peptides that bound selectively to prostate cancer cells, using *in vivo* phage display. Although the peptide bound to the prostate cancer tissue, it was also present at significant levels in the liver. Similarly, in 2011, Askoxylakis et al.,²³ using *in vivo* phage display, identified peptides that selectively bound to PC3 cells and suggested that such peptides conjugated with ¹²⁵I could be exploited for radiological diagnosis of prostate cancer. However,



the radiolabeled homing peptide bound more avidly to kidney tissue than to prostate cancer tissue. Thus, promiscuous binding to other major organs such as the liver and kidney remains a serious limitation for such peptides. On the other hand, in 2002, Arap et al.¹² performed an *in vivo* phage display in humans and identified a peptide with high binding affinity for human prostate tissue. A therapeutic construct of this peptide fused to a pro-apoptotic peptide was then administered to patients with advanced human prostate cancer. Although a certain therapeutic benefit was achieved, dose-limiting toxicity due to relatively high-grade renal dysfunction is a serious issue.²⁸ Identifying peptides that do not bind to non-diseased tissues is therefore paramount. In order to avoid the ethical concerns associated with phage display in humans, we conducted part of our study in a cynomolgus

Figure 2. Binding of Homing Peptides to LNCaP Prostate Cancer Cells

(A) LN1, LN2, and LN3 peptides modified with a biotin molecule were incubated with LNCaP cells for 24 h at a concentration of 1 $\mu\text{g}/\mu\text{L}$ and the binding affinities of the respective peptides were compared using fluorescence with Avidin D-conjugated TRITC (biotinylated peptides are stained red). Scale bars, 100 μm . (B) The percentage of TRITC-positive LNCaP cells bound with prostate cancer homing peptides ($n = 6$ per group). (C) Comparison of fluorescence intensity of each target peptide bound to LNCaP cells ($n = 6$ per group). Error bars, SD. ** $p < 0.01$.

monkey as a surrogate primate species. This approach identified peptides that do not bind to liver or kidney tissue and paves the way for investigation of novel strategies for screening effective homing peptides. We further validated our approach by showing that the homing peptides can be used to specifically target death-inducing pro-apoptotic peptides to tumor cells *in vitro* and *in vivo*.

In order to confirm the application of the identified peptide for the treatment, an experiment was conducted in which it was conjugated with a proapoptotic peptide ($\text{D}[\text{KLAKLAK}]_2$) and administered to tumor cells and tumor-bearing mice for treatment in this study. It binds to cell surface and causes cell death by disrupting mitochondrial cell membranes.²⁹ It has been reported that a concentration of approximately 300 μM is required to induce cell death, accompanied by morphological change of cells in eukaryotes when proapoptotic peptide is administered alone.¹⁹ Here, we observed cell death accompanied by a morphological change by inducing LN1-KLA peptide to prostate cancer cells and found that the LN1 peptide can efficiently transport apoptosis-inducing peptide to prostate cancer cells. Furthermore, LN1-KLA

peptide significantly inhibited tumor growth, both *in vitro* and *in vivo*, as compared to the control peptide, and it was considered to be very useful as a carrier for therapy.

We conclude that the LN1 peptide is a selective and safe carrier for various therapeutic agents and that our homing peptides screening strategy will be very useful for identifying specific carriers that can be used for drug delivery to treat multiple diseases.

MATERIALS AND METHODS

Animals

C57BL/6 mice and severe combined immunodeficient male CB17/Icr-Prkdc^{scid}/Crj (C.B-17 SCID) mice were purchased from Charles

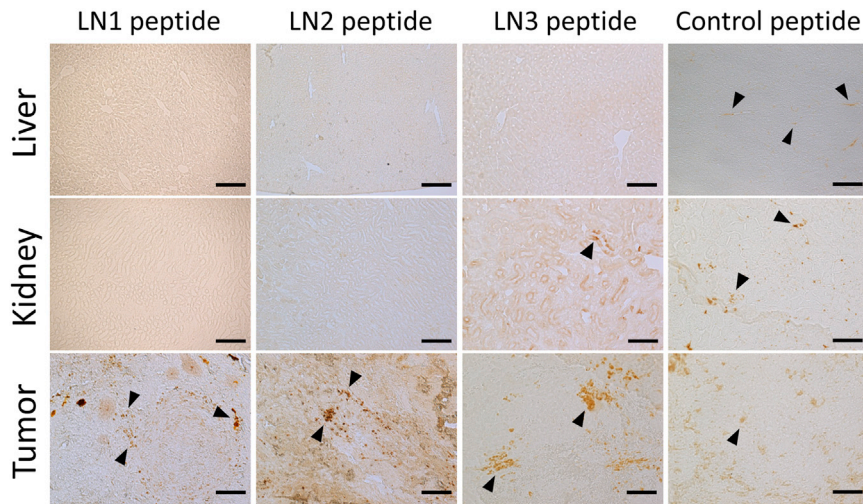


Figure 3. Histological Analysis of Homing Peptide Binding to Tumor, Liver, and Kidney Tissues in SCID Mice Bearing LNCaP Cell Xenografts

Tumor, liver, and kidney tissues were excised after each tumor-targeting peptide was administered to the tumor-implanted mouse, and DAB staining was performed. Control peptide was detected in tumor tissue and also in liver and kidney tissue. Binding of LN3 peptide was observed in tumor and kidney tissues. In contrast, LN1 and LN2 peptides were found in tumor tissue only. Arrowheads show positive staining of DAB. Scale bars, 100 μm .

River Laboratories (Osaka, Japan). The cynomolgus monkey was a gift from the Research Center for Animal Life Science in Shiga University of Medical Science.

C.B-17 SCID mice were used for all xenograft experiments with the human prostate cancer cell line. All mice were housed under standard conditions in the Institutional Animal Care and Use Committee (IACUC) at Shiga University of Medical Science and food and water were provided *ad libitum*. All animal experiments were conducted according to the guidelines of the IACUC at Shiga University of Medical Science.

Cell Culture

The human prostate cancer cell line LNCaP (RCB2144) was provided by the RIKEN BioResource Research Center (BRC) through the National BioResource Project of the Ministry of Education, Culture, Sports, Science and Technology/Japan Agency for Medical Research and Development (MEXT/AMED) (Ibaraki, Japan) and cultured in RPMI-1640 medium (Thermo Fisher Scientific, Waltham, MA, USA) with 10% fetal bovine serum (Thermo Fisher Scientific) at 37°C in an incubator with 5% CO₂ and 95% air.

LNCaP Xenograft Model in C.B-17 SCID Mice

Culture medium (250 μL) containing 2×10^6 LNCaP cells were mixed with 250 μL Matrigel (Corning, Corning, NY, USA). In order to generate prostate cancer xenografts, we injected the mixture subcutaneously into the back of 6- to 8-week-old C.B-17 SCID mice, using a 25-gauge needle. Mice were monitored weekly to monitor tumor growth.

In Vivo Phage Display and Screening of Prostate Cancer Cell Homing peptides

The M13 phage library (Ph.D.-C7C) was purchased from New England Biolabs (Ipswich, MA, USA) and was used for *in vivo* phage display to screen prostate cancer cell homing peptides. The method of phage display was performed according to the protocols described

by Christianson et al.,³⁰ with minor modifications. The phage library was injected into C57BL/6 mice through the tail vein at a titer of 1×10^9 plaque-forming units (PFU)/ μL in 100 μL Tris-buffered saline (50 mM Tris-HCl [pH7.5]). Five minutes after the injection, blood was recovered from the heart in order to remove non-specifically bound phages. The collected blood was dissolved in DMEM (Thermo Fisher Scientific) containing protease inhibitor (Sigma-Aldrich, St Louis, MO, USA). The solution was introduced into *Escherichia coli* ER2738 (New England Biolabs), and the number of phages in the blood was titrated by plaque-forming units. After amplification to 1×10^{11} PFU, the phages were injected into new C57BL/6 mice. After three rounds of *in vivo* panning with mice, the phages were injected into the femoral vein of a 15-year-old female cynomolgus monkey. Five minutes after the injection, blood was taken from the femoral vein and dissolved in DMEM with protease inhibitor. The solution was centrifuged to collect the serum, from which phages were amplified to 1×10^{11} PFU.

These phages were injected into the tail vein of a C.B-17 SCID mouse with tumor xenografts, and xenografted prostate cancer tissue was isolated after trans-cardiac removal of blood. Phages were recovered from the homogenized tissue and amplified as described above. Three additional cycles of *in vivo* phage panning were performed. After four cycles of *in vivo* panning in C.B-17 SCID mice, phage DNA was isolated from selected phage plaques with high affinity to prostate cancer tissue. The DNA sequence encoding the pIII protein was analyzed in order to identify homing peptides that localize to prostate cancer tissue.

Evaluation of Homing Peptide Binding Affinity to LNCaP Cells

In Vitro and *In Vivo*

LN1 (C-TGTPARQ-C), LN2 (C-KNSMFAT-C), and LN3 (C-TNKHSPK-C) peptides were synthesized and modified by a biotin molecule attached to their N termini (Invitrogen, Carlsbad, CA, USA). Control peptide (C-GPRTQTA-C), containing a scrambled version of the amino acid sequence of the LN1 peptide, was synthesized as a control.

For *in vitro* experiments, LNCaP cells (5×10^4 cells per well) were cultured in 24-well plates for 24 h in DMEM with 10% fetal bovine

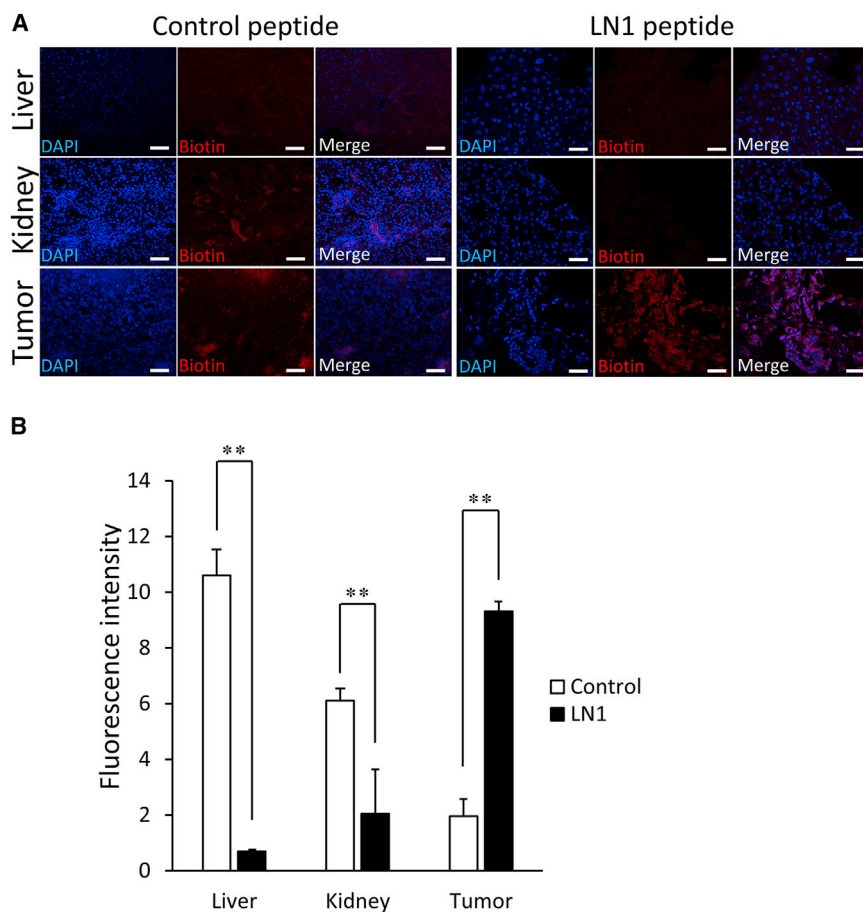


Figure 4. Quantitative Histological Analysis of LN1 Homing Peptide in Tumor Tissue

(A) The distribution of prostate cancer-specific peptide (LN1) labeled with TRITC (red) to tumor, liver, or kidney tissues 5 min after administration of LN1 peptide at a concentration of 150 μg in 100 μL PBS to tumor-bearing mice. DAPI staining of nuclei is blue. Scale bars, 50 μm . (B) Comparison of the fluorescence intensity of LN1 peptide between each tissue ($n = 3$ per group). Error bars, SD. ** $p < 0.01$.

serum. Each biotinylated peptide was added to LNCaP cells at a concentration of 1 $\mu\text{g}/\text{mL}$ in 200 μL culture medium. After incubating LNCaP cells with these peptides at 37°C for 5 min, the cells were washed with PBS, to remove the unbound biotinylated peptides, and fixed with 4% paraformaldehyde. Then each sample was blocked with PBS containing 5% normal goat serum and incubated with

after transcardial perfusion fixation with 4% paraformaldehyde. Sections prepared from liver, kidney, and tumor tissues were processed via DAB (Vector Labs, CA, USA) staining in order to evaluate the binding affinity of biotinylated peptides to these tissues *in vivo*. For fluorescent staining, the sections of prostate cancer tissue from LN1 and control groups were incubated with anti-PSA

Rhodamine Avidin D (Vector Laboratories, Burlingame, CA, USA) to visualize the biotinylated peptide. TRITC-positive cells were observed using a confocal laser microscope (FV1000-D; Olympus, Tokyo, Japan) with FLUOVIEW software version 4.01 (Olympus) and counted in each well; averages were for each peptide group. Fluorescence intensity was measured and quantified by ImageJ 1.51 (NIH, Bethesda, MD, USA). These experiments were performed in triplicate.

For *in vivo* experiments, 150 μg LN1, LN2, or LN3 peptide or control peptide was dissolved into 100 μL PBS and administered through the tail vein to individual tumor-bearing mice under general anesthesia. Five minutes after the administration, xenografted prostate cancer tissue, liver, and kidney were isolated

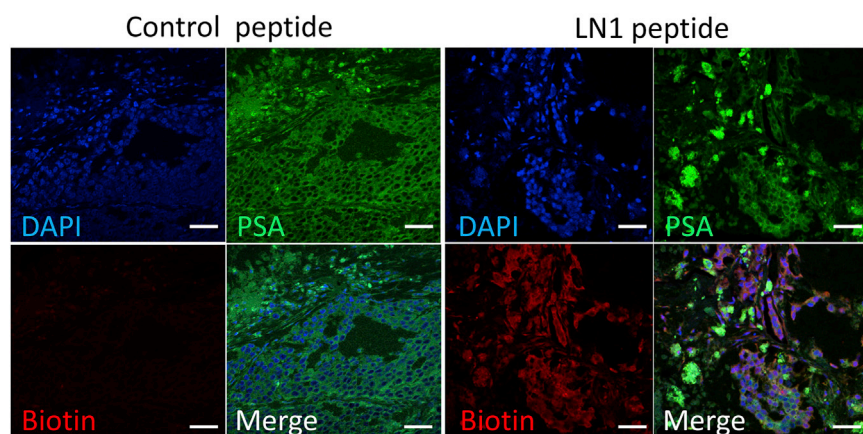


Figure 5. Immunohistochemistry of LN1 Peptide and PSA in Tumor Tissue

Analysis of LN1 peptide distribution in tumor tissue by staining control or LN1 peptide conjugated with biotin. Staining with TRITC (red) and anti-PSA antibody (green); the latter is a specific marker of prostate cancer cells. DAPI staining of nuclei is blue. Scale bars, 50 μm .

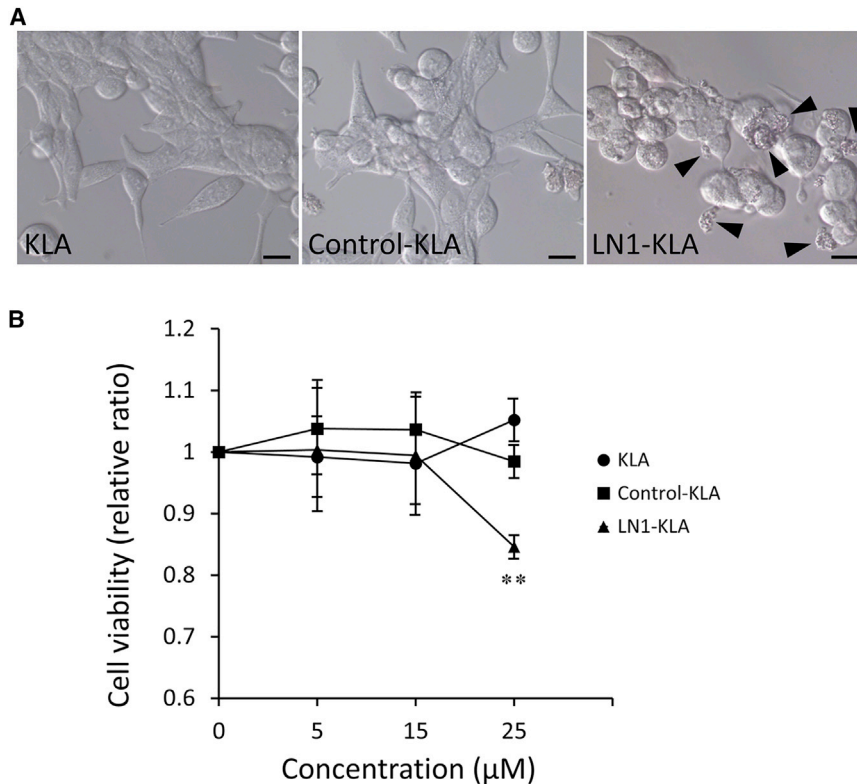


Figure 6. Apoptotic Effects of LN1-KLA Fusion Peptide in LNCaP Cells

(A) LNCaP cells were incubated with LN1-KLA peptide, KLA peptide, and control peptide for 48 h at different concentrations. Cell morphology was observed with an inverted microscope. Arrowheads show apoptotic cells. (B) Cell viability was analyzed by WST-8 assay (n = 7 per group). This ratio was compared with tumor growth in the PBS-treated group. Error bars, SD. **p < 0.01.

Treatment of Tumor-Bearing Mice with Homing Peptides

Immunodeficient mice injected under the dorsal skin with LNCaP cells were observed for approximately 2 months until tumor volume reached about 150 mm³. Then, LN1-KLA peptide, control-KLA peptide, and KLA peptide were administered via the tail vein to individual mice at a concentration of 150 µg dissolved in 100 µL PBS once every 2 days for 3 weeks.

Body weight and tumor size were measured periodically during the 3 weeks, and the tumor volume was measured using the Vevo 2100 (Visualsonics, Toronto, Canada), a small-animal imaging analysis system. This experiment

was performed with six mice in each peptide group, and tumor sizes were compared between each peptide group.

Statistical Analysis

All *in vitro* experiments were performed in triplicate. *In vivo* analyses were performed in three to six mice per group, with the exact number shown in the figure legends. Data are expressed as the mean ± standard deviation (SD). Student's t tests were performed to determine the significant differences between two groups. For multiple datasets, the differences were determined by one-way ANOVA followed by the Tukey's test. p < 0.05 was considered statistically significant.

AUTHOR CONTRIBUTIONS

A.W. performed the experiments, statistically analyzed the data, and drafted the manuscript. T.T. advised on the experimental procedures, designed the study, and helped to draft and revise the manuscript. H.K. and S.K. advised on experimental design and techniques and revised the manuscript. A.K., M.N., and T.Y. provided expertise and feedback. All authors read and approved the final manuscript.

CONFLICTS OF INTEREST

The authors declare no competing interests.

ACKNOWLEDGMENTS

We gratefully acknowledge the work of all those who helped us during this study. We would like to thank the Central Research Laboratory,

primary antibody (GeneTex, Irvine, CA, USA) overnight at 4°C. After the primary antibody was washed out, those sections were incubated with species-matched AlexaFluor-488 conjugated secondary antibody (Thermo Fisher Scientific) and Rhodamine Avidin D. Sections of liver and kidney tissues from the LN1 and control groups were also incubated with Rhodamine Avidin D. All sections were observed using a confocal laser microscope (C1si; Nikon, Tokyo, Japan), with EZC1 software version 3.90 (Nikon). Fluorescence intensity was measured and quantified by ImageJ 1.51 (NIH, Bethesda, MD, USA). *In vivo* experiments were conducted using three mice in each peptide group.

Cell Viability Assay

C-TGTPARQ-C (LN1)-GGG-D(KLAKLAK)₂ (LN1-KLA peptide), C-GPRTQTA-C (control peptide)-GGG-D(KLAKLAK)₂ (control-KLA peptide), and D(KLAKLAK)₂ (KLA peptide) were synthesized by Invitrogen (Carlsbad, CA, USA). LN1 or control peptide and proapoptotic peptide (D[KLAKLAK]₂) were linked by a glycyl-glycyl-glycine bridge. Therefore, homing peptide (LN1 or control) and D(KLAKLAK)₂ domains could independently move around the glycine bridge, because the glycine residue has no polarity. LNCaP cells were seeded in 96-well plates at a density of 1 × 10⁴ cells per well and cultured in RPMI-1640 medium with 10% fetal bovine serum 24 h before the assay. The cells were incubated with different concentrations of the LN1-KLA fusion peptide, the control-KLA fusion peptide, or the KLA peptides for 48 h. Cell viability was measured using the WST8 assay (Dojindo, Kumamoto, Japan).

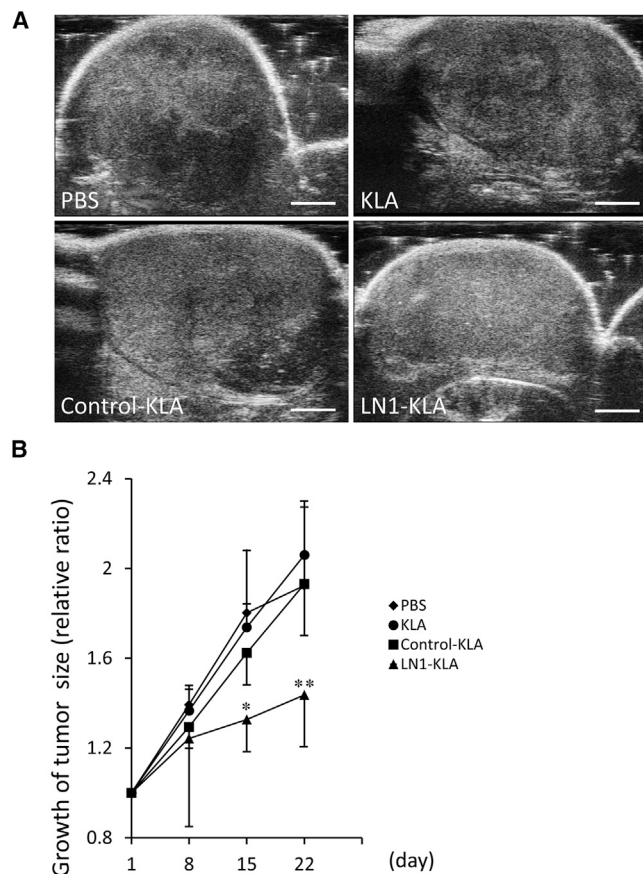


Figure 7. Inhibition of LNCaP Xenograft Growth by LN1-KLA Peptide Treatment

(A) Ultrasound images of tumors in PBS, KLA, Control-KLA, and LN1-KLA groups on day 22 after treatment. Scale bars, 2 mm. (B) Tumor size was measured, and the volume of each tumor was calculated by using the Vevo 2100 system. Tumor growth rates were compared between each treatment peptide group ($n = 6$ per group). Error bars, SD. * $p < 0.05$; ** $p < 0.01$.

Shiga University of Medical Science, for technical support. This work was supported by Japan Society for the Promotion of Science (JSPS) KAKENHI grant number JP16K11001.

REFERENCES

- Cornford, P., Bellmunt, J., Bolla, M., Briers, E., De Santis, M., Gross, T., Henry, A.M., Joniau, S., Lam, T.B., Mason, M.D., et al. (2017). EAU-ESTRO-SIOG Guidelines on Prostate Cancer. Part II: Treatment of relapsing, metastatic, and castration-resistant prostate cancer. *Eur. Urol.* *71*, 630–642.
- Harris, W.P., Mostaghel, E.A., Nelson, P.S., and Montgomery, B. (2009). Androgen deprivation therapy: progress in understanding mechanisms of resistance and optimizing androgen depletion. *Nat. Clin. Pract. Urol.* *6*, 76–85.
- Nevedomskaya, E., Baumgart, S.J., and Haendler, B. (2018). Recent advances in prostate cancer treatment and drug discovery. *Int. J. Mol. Sci.* *19*, e1359.
- de Bono, J.S., Oudard, S., Ozguroglu, M., Hansen, S., Machiels, J.P., Kocak, I., Gravis, G., Bodrogi, I., Mackenzie, M.J., Shen, L., et al.; TROPIC Investigators (2010). Prednisone plus cabazitaxel or mitoxantrone for metastatic castration-resistant prostate cancer progressing after docetaxel treatment: a randomised open-label trial. *Lancet* *376*, 1147–1154.
- Fizazi, K., Scher, H.I., Molina, A., Logothetis, C.J., Chi, K.N., Jones, R.J., Staffurth, J.N., North, S., Vogelzang, N.J., Saad, F., et al.; COU-AA-301 Investigators (2012). Abiraterone acetate for treatment of metastatic castration-resistant prostate cancer: final overall survival analysis of the COU-AA-301 randomised, double-blind, placebo-controlled phase 3 study. *Lancet Oncol.* *13*, 983–992.
- Beer, T.M., Armstrong, A.J., Rathkopf, D.E., Loriot, Y., Sternberg, C.N., Higano, C.S., Iversen, P., Bhattacharya, S., Carles, J., Chowdhury, S., et al.; PREVAIL Investigators (2014). Enzalutamide in metastatic prostate cancer before chemotherapy. *N. Engl. J. Med.* *371*, 424–433.
- Pasqualini, R., Koivunen, E., and Ruoslahti, E. (1997). Alpha v integrins as receptors for tumor targeting by circulating ligands. *Nat. Biotechnol.* *15*, 542–546.
- Tai, W., Mahato, R., and Cheng, K. (2010). The role of HER2 in cancer therapy and targeted drug delivery. *J. Control. Release* *146*, 264–275.
- Terashima, T., Oka, K., Kritiz, A.B., Kojima, H., Baker, A.H., and Chan, L. (2009). DRG-targeted helper-dependent adenoviruses mediate selective gene delivery for therapeutic rescue of sensory neuropathies in mice. *J. Clin. Invest.* *119*, 2100–2112.
- Terashima, T., Ogawa, N., Nakae, Y., Sato, T., Katagi, M., Okano, J., Maegawa, H., and Kojima, H. (2018). Gene therapy for neuropathic pain through siRNA-IRF5 gene delivery with homing peptides to microglia. *Mol. Ther. Nucleic Acids* *11*, 203–215.
- Kolonin, M., Pasqualini, R., and Arap, W. (2001). Molecular addresses in blood vessels as targets for therapy. *Curr. Opin. Chem. Biol.* *5*, 308–313.
- Arap, W., Kolonin, M.G., Trepel, M., Lahdenranta, J., Cardó-Vila, M., Giordano, R.J., Mintz, P.J., Ardel, P.U., Yao, V.J., Vidal, C.I., et al. (2002). Steps toward mapping the human vasculature by phage display. *Nat. Med.* *8*, 121–127.
- Smith, G.P., and Petrenko, V.A. (1997). Phage display. *Chem. Rev.* *97*, 391–410.
- Giordano, R.J., Cardó-Vila, M., Lahdenranta, J., Pasqualini, R., and Arap, W. (2001). Biopanning and rapid analysis of selective interactive ligands. *Nat. Med.* *7*, 1249–1253.
- Shukla, G.S., and Krag, D.N. (2005). Phage display selection for cell-specific ligands: development of a screening procedure suitable for small tumor specimens. *J. Drug Target.* *13*, 7–18.
- Koivunen, E., Arap, W., Rajotte, D., Lahdenranta, J., and Pasqualini, R. (1999). Identification of receptor ligands with phage display peptide libraries. *J. Nucleic Med.* *40*, 883–888.
- Pasqualini, R., and Ruoslahti, E. (1996). Organ targeting in vivo using phage display peptide libraries. *Nature* *380*, 364–366.
- Arap, W., Pasqualini, R., and Ruoslahti, E. (1998). Cancer treatment by targeted drug delivery to tumor vasculature in a mouse model. *Science* *279*, 377–380.
- Ellerby, H.M., Arap, W., Ellerby, L.M., Kain, R., Andrusiak, R., Rio, G.D., Krajewski, S., Lombardo, C.R., Rao, R., Ruoslahti, E., et al. (1999). Anti-cancer activity of targeted pro-apoptotic peptides. *Nat. Med.* *5*, 1032–1038.
- Yao, V.J., Ozawa, M.G., Trepel, M., Arap, W., McDonald, D.M., and Pasqualini, R. (2005). Targeting pancreatic islets with phage display assisted by laser pressure catapult microdissection. *Am. J. Pathol.* *166*, 625–636.
- Arap, W., Haedicke, W., Bernasconi, M., Kain, R., Rajotte, D., Krajewski, S., Ellerby, H.M., Bredesen, D.E., Pasqualini, R., and Ruoslahti, E. (2002). Targeting the prostate for destruction through a vascular address. *Proc. Natl. Acad. Sci. USA* *99*, 1527–1531.
- Newton, J.R., Kelly, K.A., Mahmood, U., Weissleder, R., and Deutscher, S.L. (2006). *In vivo* selection of phage for the optical imaging of PC-3 human prostate carcinoma in mice. *Neoplasia* *8*, 772–780.
- Askoxylakis, V., Zitzmann-Kolbe, S., Zoller, F., Altmann, A., Markert, A., Rana, S., Marr, A., Mier, W., Debus, J., and Haberkorn, U. (2011). Challenges in optimizing a prostate carcinoma binding peptide, identified through the phage display technology. *Molecules* *16*, 1559–1578.
- Sobel, R.E., and Sadar, M.D. (2005). Cell lines used in prostate cancer research: a compendium of old and new lines: part 2. *J. Urol.* *173*, 360–372.
- Sobel, R.E., and Sadar, M.D. (2005). Cell lines used in prostate cancer research: a compendium of old and new lines: part 1. *J. Urol.* *173*, 342–359.

26. Qin, B., Tai, W., Shukla, R.S., and Cheng, K. (2011). Identification of a LNCaP-specific binding peptide using phage display. *Pharm. Res.* 28, 2422–2434.
27. Jayanna, P.K., Bedi, D., Deinnocentes, P., Bird, R.C., and Petrenko, V.A. (2010). Landscape phage ligands for PC3 prostate carcinoma cells. *Protein Eng. Des. Sel.* 23, 423–430.
28. Pasqualini, R., Millikan, R.E., Christianson, D.R., Cardó-Vila, M., Driessen, W.H., Giordano, R.J., Hajitou, A., Hoang, A.G., Wen, S., Barnhart, K.F., et al. (2015). Targeting the interleukin-11 receptor α in metastatic prostate cancer: A first-in-man study. *Cancer* 121, 2411–2421.
29. Mai, J.C., Mi, Z., Kim, S.H., Ng, B., and Robbins, P.D. (2001). A proapoptotic peptide for the treatment of solid tumors. *Cancer Res.* 61, 7709–7712.
30. Christianson, D.R., Ozawa, M.G., Pasqualini, R., and Arap, W. (2007). Techniques to decipher molecular diversity by phage display. *Methods Mol. Biol.* 357, 385–406.